Coulomb-nuclear interference and extraction of nuclear parameters

K. M. Das and B. B. Deo
Department of Physics, Utkal University, Bhubaneswar-751004, India
(Received 5 March 1981)

A novel method of separating strong and electromagnetic contributions to the charge particle scattering on nuclei is presented. Data from nonforward angles are extrapolated to the forward angle to obtain the residue of the Coulomb pole which is proportional to the forward nuclear amplitude $f_N(0)$. Except for the treatment of the Coulombic effects, the method is model independent. Optical polynomial expansion is used to improve the goodness of the fits. Reliable values of the total elastic, total inelastic, and total nuclear scattering cross sections can be obtained. The method is applied to study the elastic scattering of charged pions from ^{4}He nuclei. The differential cross-section results of Binon *et al.* at five energies ranging from 110 to 260 MeV and of Crowe *et al.* at four energies ranging from 51 to 75 MeV are separately analyzed. The extracted results agree, not only with those of Binon *et al.*, but also with the values of real parts of the forward scattering amplitude obtained by Wilkin *et al.* and Batty *et al.* using forward dispersion relations.

[NUCLEAR REACTIONS ^{4}He($\pi^\pm,\pi^\pm$), $T^{\rm lab}=51-75$ MeV; ^{4}He(π^-,π^-), $T^{\rm lab}=110-260$ MeV; calculated forward nuclear amplitudes, elastic, inelastic, total σ; pole extrapolation method.]

I. INTRODUCTION

Several attempts have been made in the past for isolating the complex nuclear amplitude at forward angles from the differential cross-section data for elastic scattering of charged pions from nuclei. The imaginary part is usually obtained from the total cross section using the optical theorem. The real part is obtained by one of the following methods:

(a) for neutral pions, from a forward differential cross section,

$$\frac{d\sigma}{d\Omega}(0^\circ)=\mathrm{Re}f_N(0)^2+\mathrm{Im}f_N(0)^2\ ; \tag{1}$$

(b) through the use of forward dispersion relations[1–3];

(c) by a phase-shift analysis[4,5];

(d) by phenomenological fits to experimental data in the Coulomb-nuclear interference region.[6–8]

The first method, applicable in restricted cases, does not even provide the exact sign of $\mathrm{Re}f_N(0)$. Forward dispersion relations have been used by Ericson and Locher[1] to calculate the real parts of the "symmetric amplitude." In the more recent calculations by Wilkin *et al.*[2] and Batty *et al.*,[3] significant variations in the values obtained for the real parts have been reported, because accurate values of the total cross sections in the entire energy range of interest for the dispersion integrals are not available. There are also uncertainties in the values used for subtraction constants in the dispersion relations.

Falomkin *et al.*[4] have made a phase-shift analysis to obtain the forward pion-^{4}He amplitude. In spite of the improvements suggested by Dumbrais *et al.*,[5] the methods based on phase-shift analysis still involve too many parameters and are ridden with ambiguities.

More recently, real parts of the forward nuclear amplitude have been obtained by Binon *et al.*[6,7] and Scott *et al.*[8] They have performed a fit to the differential cross-section data in the Coulomb-interference region with a semiphenomenological expression

$$\frac{d\sigma}{d\Omega}(\theta)=|f_{\rm Coul}(\theta)e^{2i\phi}+f_N(\theta)|^2\ , \tag{2}$$

where $f_{\rm Coul}(\theta)$ and $f_N(\theta)$ are the Coulomb and nuclear amplitudes, respectively. The relative Bethe phase 2ϕ has been taken as[9]

$$2\phi=-2\xi\ln\sin\tfrac{1}{2}\theta+\xi\int_{-4k^2}^{0}\frac{dt}{|t'-t|}\left[1-\frac{f_N(t')}{f_N(t)}\right], \tag{3}$$

the coupling parameter ξ being related to the fine structure constant α as

$$\xi=\frac{Z_1Z_2\alpha[s-(m^2+M^2)]}{[s-(m+M)^2]^{1/2}[s-(m-M)^2]^{1/2}} . \quad (4)$$

k is the center of mass (c.m.) momentum; s and t are the usual Mandelstam variables; Z_1, Z_2 are the charges; and m and M are the masses of the projectile and target, respectively. For evaluating the integral in Eq. (3), an exponential form for the nuclear amplitude has been used. This assumes diffraction scattering ignoring, for instance, the existence of a forward dip. Binon also uses a phenomenological expression for $f_N(\theta)$ in Eq. (2) which is diffractive and is not of the correct form for all values of $\cos\theta$ from -1 to $+1$.

Thus, the above methods use assumed nuclear models to fit the experimental data. We also feel that they use too many parameters. The objective of the present paper is, therefore, twofold. The first is to suggest a novel method to obtain the nuclear amplitudes in the forward direction, where no specific nuclear model will be used. One will then obtain unbiased estimates of the nuclear parameters. The second is to use conformal mapping to achieve accelerated convergence of the series representations so that the goodness of the fits increases optimally and the number of parameters in the fits is reduced considerably. The conformal mapping technique has been largely used in nuclear physics for extrapolation to unphysical regions. Kisslinger[10] and Dubnička *et al.*[5,10] have used it to obtain coupling constants and phase shifts. Kisslinger and Nichols[11] were the first to use the optimal expansion technique for nuclear scattering in the $\cos\theta$ plane allowing for the effects of Coulomb distortion on spectroscopic factors.

Since for charged particle scattering there is a Coulomb pole at $t=0$, its contribution to the scattering amplitude has to be first subtracted out to obtain reliable information about the forward nuclear amplitude. The data from nonforward angles have to be suitably and stably extrapolated to the inaccessible forward point $t=0$. An elegant method of such a pole extrapolation has been suggested by Cutkosky and Deo[12] which can be easily adopted for the present problem. After subtraction of the Coulomb part, the remaining nuclear part is conveniently parametrized in conformally mapped variables dictated by the analyticity of the strong interaction amplitude.

Recent experimental results of negative pion scattering from ^{4}He nuclei in the Coulomb interference region[7] provide an excellent set of data to carry out this intended analysis and to assess the merits and workability of the method. The data extend over a wide range of angles from near forward to the very backward region between 110 to 260 MeV. The real parts, both in sign and magnitude, are obtained quite neatly as residues by extrapolation to the forward pole. In fact, the present method provides a direct experimental proof of the existence of a first order Coulombic pole in the forward direction in the interference term. The total cross section is also found from the imaginary part obtained by a method of successive iteration.

The paper is divided into six sections. In Sec. II, the equations for analyzing pion-nucleus scattering are presented. Section III deals with the main extrapolation procedure. The methods for obtaining various nuclear data from the measured differential cross sections are also given here. In Sec. IV, analytic structure of the nuclear amplitude and elliptic mapping are briefly discussed. In Sec. V, we present the extrapolation procedure for a lower energy and wider angle to treat the experimental data of Ref. 13. Section VI contains a discussion of our results.

II. PION-NUCLEUS SCATTERING

Formally, the scattering amplitude is given by

$$f(\theta)=\sum_{l=0}^{\infty}\frac{2l+1}{2ik}(e^{2i\delta_l}-1)P_l(\cos\theta) . \quad (5)$$

For a Coulomb plus a short range nuclear force,[14] the phase shift δ_l is the sum of the Coulomb phase shift σ_l, the nuclear phase shift ν_l, and a suitable matching phase angle λ_l, given as

$$\lambda_l\approx\begin{cases}-\sigma_l , & l>>kb\\ -\xi\ln(2kb)=\lambda , & l<<kb ,\end{cases} \quad (6)$$

b being of the order of the range of nuclear interaction. The Coulomb phase shift is

$$\sigma_l=\frac{1}{2i}\ln\frac{\Gamma(l+1+i\xi)}{\Gamma(l+1-i\xi)} . \quad (7)$$

The full amplitude is written as

$$f(\theta)=f_{sp}(\theta)+e^{2i\lambda}[f_c(\theta)+f_N(\theta)] , \quad (8)$$

where

$$f_c(\theta)=\sum_{l=0}^{\infty}\frac{2l+1}{2ik}(e^{2i\sigma_l}-1)P_l(\cos\theta)\ , \tag{9}$$

$$f_N(\theta)=\sum_{l=0}^{\infty}\frac{2l+1}{2ik}e^{2i\sigma_l}(e^{2i\nu_l}-1)P_l(\cos\theta)\ , \tag{10}$$

$$f_{sp}(\theta)=\sum_{l=0}^{\infty}\frac{2l+1}{2ik}[(e^{2i\lambda}-1)+e^{2i\sigma_l}(e^{2i\lambda_l}-e^{2i\lambda})]P_l(\cos\theta)\ . \tag{11}$$

The Coulomb amplitude is taken to be

$$f_c(\theta)=f_c^B e^{2i[\sigma_0-\xi\ln\sin(1/2)\theta]}\ , \tag{12}$$

where

$$f_c^B=\frac{2\xi k}{t}\ . \tag{13}$$

For scattering of strongly interacting particles at angles $\theta>>1/kb\approx10^{-5}$ radians, f_{sp} is certainly negligible.[14] One can also show that the contribution of f_{sp} is of the order of α^3 and is inaccessible to this analysis. Effectively, then,

$$\frac{d\sigma}{d\Omega}(\theta)=|f(\theta)|^2$$

$$\approx|f_c(\theta)+f_N(\theta)|^2\ . \tag{14}$$

Equation (14) is to be compared with the expression (2) used by Binon. Theoretically, they should lead to equal values of the residues at fixed energy to the order α^2, if the nuclear model used has been correct.

If we consider the finite sizes of the incident and target particles, the above Coulomb amplitude gets modified[15] and equals

$$\{f_c(\theta)-f_c^B[1-F(\theta)]\}\ ,$$

$F(\theta)$ being the electromagnetic form factor. As is evident from Eq. (10), the amplitude $f_N^{\pm}(\theta)$ is not purely nuclear, but is distorted by the Coulomb phase factor. Hence, the scattering cross section for $\pi^{\pm}$ scattered from ^{4}He nuclei is

$$\frac{d\sigma^{\pm}}{d\Omega}(\theta)=|f_c(\theta)-f_c^B[1-F(\theta)]|^2+|f_N^{\pm}(\theta)|^2\pm2\{\mathrm{Re}f_c(\theta)-f_c^B[1-F(\theta)]\}\,\mathrm{Re}f_N^{\pm}(\theta)$$

$$+2\,\mathrm{Im}f_c(\theta)\,\mathrm{Im}f_N^{\pm}(\theta)\ , \tag{15}$$

where $f_N^{\pm}(\theta)$ refers to the residual nuclear amplitude for $\pi^{\pm}$.

We use the product $F_\pi(t)F_{^4\mathrm{He}}(t)$ for the em form factor $F(\theta)$, in which

$$F_\pi(t)=\exp(-r_\pi{}^2|t|/6)\ , \tag{16}$$

$$F_{^4\mathrm{He}}(t)=\exp(-r_{^4\mathrm{He}}{}^2|t|/6)\ , \tag{17}$$

r_π and $r_{^4\mathrm{He}}$ being the charge radii of pion and helium nucleus, respectively. The effects of these terms are found to be negligible. The terms are, however, included with acceptable values of the radii: $r_\pi=0.8$ fm and $r_{^4\mathrm{He}}=1.67$ fm.

III. EXTRAPOLATION PROCEDURE

The scattering cross section, as represented by Eq. (15), contains both first and second order electromagnetic poles at $t=0$. There is also the cut from $t=0$ to ∞. The contribution from the pure Coulomb term containing the second order pole is known. The Coulomb-nuclear interference terms contain the first order $t=0$ pole and are of significance here. The strength of this singularity at $t=0$ is proportional to the real and/or imaginary parts of the forward nuclear amplitude. The pole is on the forward edge of the physical region and the contribution of the interference terms in the forward

angles is comparable with the nuclear contribution itself. So the pole extrapolation here is a powerful method for determining the nuclear parameters to a high degree of accuracy.

Another significant factor is that no exact nuclear model is needed for such analysis. The interference terms having been determined and subtracted out, the differential cross section for the strong interaction can be obtained for all scattering angles. However, a word of caution is necessary. Sometimes the extrapolation may not be very stable due to non-negligible contributions from the electromagnetic cut, especially at low energies.

Details of the extrapolation procedure are outlined below:

With the Coulomb singularities and cuts from $t=0$, the differential scattering cross section is not analytic, and hence, no classical polynomial expansion will converge. We assume that the pole and the cut, to order α, are given accurately by the generalization of the nonrelativistic theory as given by Eq. (12). Only when the singular terms are accurately subtracted from the data, can the remainder be expanded in a convergenet series of orthogonal polynomials. The region of convergence will then be the ellipse contained by the nearest singularity in the $\cos\theta$ plane. To explain further, let us write the singularity-subtracted differential cross section $\mathcal{F}(s,\theta)$ as

$$\mathcal{F}(s,\theta)=\frac{d\sigma}{d\Omega}(\theta)\Big|_{\text{exp}}-(\,|f_c(\theta)-f_c^B[1-F(\theta)]\,|^2\pm 2\{\,\mathrm{Re}f_c(\theta)-f_c^B[1-F(\theta)]\,\}\,\mathrm{Re}f_N^{\pm}(0)$$
$$+2\,\mathrm{Im}f_c(\theta)\,\mathrm{Im}f_N^{\pm}(0))\,. \tag{18}$$

The first term inside the bold parentheses is the pure Coulomb contribution and it contains the second order pole at $t=0$. The second term, containing the simple pole at $t=0$, is due to Coulomb-nuclear interference. So these terms are very important for us. The last term is dominated by the weak electromagnetic cut.

The quantity $\mathcal{F}(s,\theta)$ can be expanded in a series such as

$$\mathcal{F}(s,\theta)=\sum_n a_n(s)p_n(\cos\theta)\,, \tag{19}$$

where the polynomials p_n are weighted by the experimental errors in the differential cross sections and are constructed by Schmidt's orthogonalization procedure. From a fit to the data, with a series of L terms, the ${\chi_L}^2$ value obtained is

$${\chi_L}^2=\sum_i\left[\frac{\mathcal{F}_i-\sum_{n=1}^{L}a_np_n(\cos\theta_i)}{\Delta W_i}\right]^2, \tag{20}$$

ΔW_i being the error in the differential cross section at $\cos\theta_i$. In case Coulomb singularities are not exactly substracted, $\mathcal{F}(s,\theta)$ will contain Coulomb pole terms and the polynomial expansion (19) will not converge. As a result of nonconvergence, χ^2 will be large for any given order of truncation of the expansion. With correct subtraction of the poles, the χ^2 value will be reduced to a minimum. Thus, at the correct subtraction point, χ^2 will show a pronounced dip as the strength of the singularity is varied. The more accurate the data, the sharper the dip. The expansion must also be optimal, embracing the entire domain of analyticity as the region of convergence for the least χ^2.

Once the Coulomb pole terms have been correctly subtracted, $\mathcal{F}(s,\theta)$ is mostly the nuclear differential scattering cross section. However, there are two unknown residues $\mathrm{Re}f_N(0)$ and $\mathrm{Im}f_N(0)$. They have to be found simultaneously. Because of the lack of a distinct pole in the imaginary part of the Coulomb amplitude, a substantial variation in the nuclear imaginary part does not appear to affect the extrapolation. So it is possible to use the extrapolation in an iterative manner, taking advantage of the relation

$$|f_N(0)|^2=\frac{d\sigma_N}{d\Omega}(0^\circ)$$
$$=|\,\mathrm{Re}f_N(0)\,|^2+|\,\mathrm{Im}f_N(0)\,|^2\,. \tag{21}$$

For a certain value of $\mathrm{Re}f_N(0)$, the iteration is started by taking some plausible value of the imaginary part in the residue term of Eq. (18). $\mathcal{F}(s,\theta)$ is now extrapolated through the polynomials to give $d\sigma_N/d\Omega$ at $\theta=0^\circ$. A fresh value for $\mathrm{Im}f_N(0)$ is obtained from relation (21). This new value of $\mathrm{Im}f_N(0)$ is now fed back in the residue term and

the extrapolation procedure is repeated. This is continued until stable values of $d\sigma_N/d\Omega(0°)$ and $\mathrm{Im}f_N(0)$ are obtained. Table I shows a typical cycle of iteration of 110 MeV for one value of $\mathrm{Re}f_N(0)$. The fits are, of course, carried out for different values of $\mathrm{Re}f_N(0)$ to obtain the minimum of the χ^2 curve. It is found that quite accurate values of $\mathrm{Im}f_N(0)$ are obtained by this method of iteration with constraint (21).

Correctly subtracted for the value of the residue when χ^2's are minima, the remainder

$$\mathscr{F}_0(s,\theta)=\sum_n a_n p_n(\cos\theta) \tag{22}$$

is extrapolated to $\theta=0°$. It is also integrated graphically to obtain the total elastic cross section. The total cross section is calculated from the relation

$$\sigma_{\mathrm{tot}}=\frac{4\pi}{k}\,\mathrm{Im}f_N(0)\ . \tag{23}$$

The total inelastic cross section is obtained as the difference of the previous two cross sections.

IV. ANALYTIC STRUCTURE OF NUCLEAR SCATTERING AMPLITUDE AND ELLIPTIC MAPPING

The rate of convergence of the polynomial expansion of $\mathscr{F}(s,\theta)$ is determined by the singularity structure of the scattering amplitude due to strong interactions. The nuclear part of the $\pi^{\pm}$-^{4}He scattering amplitude is free from poles in both direct and cross channels. The t-channel singularity begins with the two pion exchange. The right-hand cut, in the $\cos\theta$ plane (x plane), extends from

$$x_+=1+\frac{2m_{\pi^0}{}^2}{k^2} \tag{24}$$

TABLE I. A typical cycle of iteration at 110 MeV for $\mathrm{Re}f_N(0)=1.2$ fm and $L=7$, starting with $\mathrm{Im}f_N(0)=1.5$ fm.

No. of iteration	$\frac{d\sigma_N}{d\Omega}(0°)$ (mb/sr)	$\mathrm{Im}f_N(0)$ (fm)	χ^2
1	45.34	1.759	56.93
2	45.59	1.766	56.76
3	45.60	1.766	56.76
4	45.60 (stable)	1.766 (stable)	56.76

to infinity. The u-channel singularity is the left-hand cut extending from $-x_-$, the threshold for production of ^{3}He (^{3}H) and $p(n)$ in the u channel, to $-\infty$.

$$x_-=1+\frac{[m_{^3\mathrm{He}(^3\mathrm{H})}+m_{p(n)}]^2}{2k^2} -\frac{[m_{\pi^\pm}{}^2-m_{^4\mathrm{He}}{}^2]^2}{2k^2 s}\ . \tag{25}$$

The full assumed analytic structure of $\mathscr{F}(s,\theta)$ is shown in Fig. 1.

The polynomial series (22) converges within the Lehmann ellipse[16] touching the right-hand cut at x_+. To optimize the rate of convergence of the polynomial expansion, the $\cos\theta$ plane is mapped into the interior of an ellipse,[17] the cuts lying on the boundary of the ellipse in a mapped (z) plane. The mapping is performed in two steps. First, the cuts $(-\infty,-x_-)$ and (x_+,∞) are symmetrized to $(-\infty,-W)$ and (W,∞), respectively, by a transformation

$$w=\frac{x-x_0}{1-xx_0}\ , \tag{26}$$

where

$$x_0=\frac{x_--x_+}{x_+x_-+X_+X_--1}\ , \tag{27}$$

$$W=\frac{x_+X_-+x_-X_+}{X_++X_-}\ , \tag{28}$$

and $X_\pm=(x_\pm{}^2-1)^{1/2}$. Next, the symmetrized cuts are mapped onto an ellipse by

$$z=\sin[\tfrac{1}{2}F(\sin^{-1}w,k)/K(k)]\ , \tag{29}$$

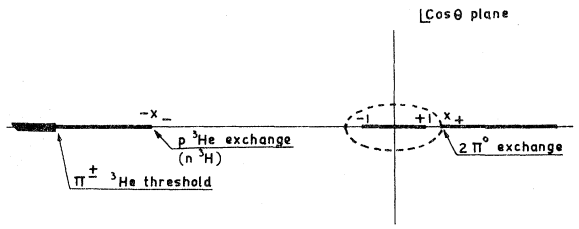

FIG. 1. Analytic structure of $\pi^{\pm}$-^{4}He scattering amplitudes in $\cos\theta$ plane. The dashed line ellipse is the ellipse of convergence (see text) with x_+ as the semimajor axis.

where $k=1/W$, and $K(k)$ and $F(\phi,k)$ are the complete and incomplete elliptic integrals of the first kind.

Table II shows the size of the new ellipse, which is quite large compared to the normal Lehmann ellipse. Orthogonal polynomials $P_n(z)$ are constructed in the new z variable and the quantity $\mathcal{F}(s,\theta)$ is fitted in a series $\sum_n b_n P_n(z)$ to obtain the χ^2 values.

χ^2 curves for the real part of the forward amplitude at five different energies between 110 and 260 MeV are displayed in Fig. 2. The minima of these curves correspond to the extracted values of $\mathrm{Re}f_N^-(0)$.

V. EXTRAPOLATION PROCEDURE FOR DATA AWAY FROM THE FORWARD REGION

The method discussed in Sec. III is slightly modified for analyzing the data of Crowe *et al.* at low energies. The experiments have been performed far away from the forward region, i.e., at $\theta\approx 30°-150°$. Most of the fits required about four to five order polynomials in the expansion and preliminary fits gave very high χ^2 values. So we concluded that extrapolation from $\theta\approx 30°$ to $\theta=0°$ has become unreliable. Quite fortunately, there are differential cross-section data for both π^+ and π^- at the same angles. It is possible to fit the sum and the difference of the differential cross sections separately. This results in a much better and more accurate analysis. The sum

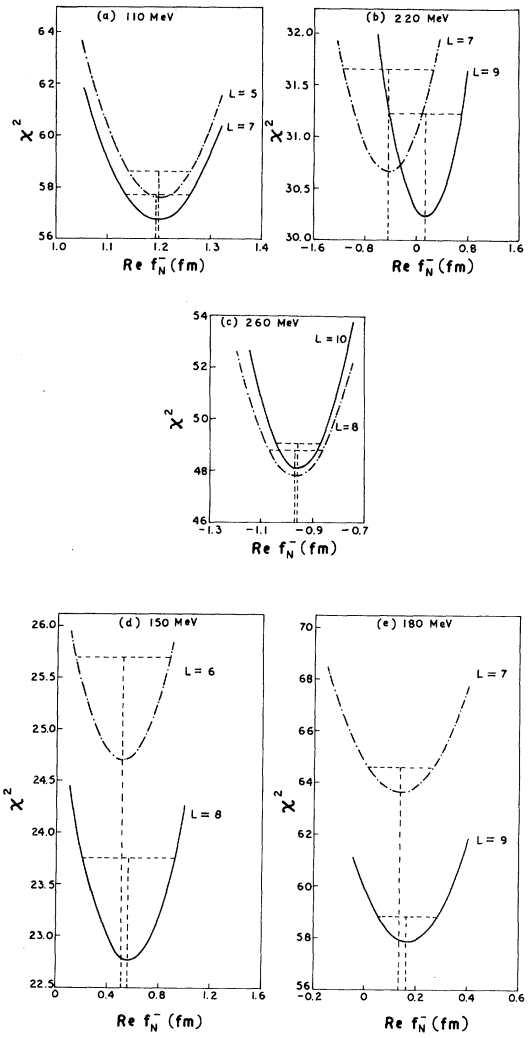

FIG. 2. Plot of χ^2 against different values of $\mathrm{Re}f_N^-(0)$. Solid (——) curves for the x plane; dotted-dashed (—·—·—) curves for the z plane; and L = order of the polynomial where the series is truncated.

TABLE II. T^{lab} = pion kinetic energy in the laboratory, x_+ = semimajor axis of the Lehmann ellipse, and a = semimajor axis of the Cutkosky-Deo ellipse.

T^{lab} (MeV)	x_+	a
51	3.389	12.385
60	2.985	10.812
68	2.718	9.768
75	2.532	9.034
110	1.966	6.748
150	1.655	5.430
180	1.517	4.821
220	1.396	4.259
260	1.316	3.867

$$\frac{d\sigma_N^-}{d\Omega}(\theta)+\frac{d\sigma_N^+}{d\Omega}(\theta)=\left[\frac{d\sigma^-}{d\Omega}(\theta)+\frac{d\sigma^+}{d\Omega}(\theta)\right]_{\mathrm{exp}}$$
$$-2\,|f_c(\theta)-f_c^B[1-F(\theta)]\,|^2$$
$$+2[\mathrm{Re}f_c(\theta)-f_c^B[1-F(\theta)]$$
$$\times[\mathrm{Re}f_N^-(0)-\mathrm{Re}f_N^+(0)]$$
$$-2\,\mathrm{Im}f_c(\theta)[\mathrm{Im}f_N^-(0)$$
$$+\mathrm{Im}f_N^+(0)] \quad (30)$$

and the difference

$$\frac{d\sigma_N^-}{d\Omega}(\theta)-\frac{d\sigma_N^+}{d\Omega}(\theta)=\left[\frac{d\sigma^-}{d\Omega}(\theta)-\frac{d\sigma^+}{d\Omega}(\theta)\right]_{\text{exp}}$$
$$+2[\mathrm{Re}f_c(\theta)-f_c^B(1-f(\theta))]$$
$$\times[\mathrm{Re}f_N^-(0)+\mathrm{Re}f_N^+(0)]$$
$$-2\,\mathrm{Im}f_c(\theta)[\mathrm{Im}f_N^-(0)-\mathrm{Im}f_N^+(0)] \quad (31)$$

both contain the pole at $t=0$.

If the poles are correctly subtracted, the sum and the difference can be separately fitted to the set of constructed orthogonal polynomials. Now, if we write $\mathcal{F}_\pm(s,\theta)$ for the sum or the difference, it can

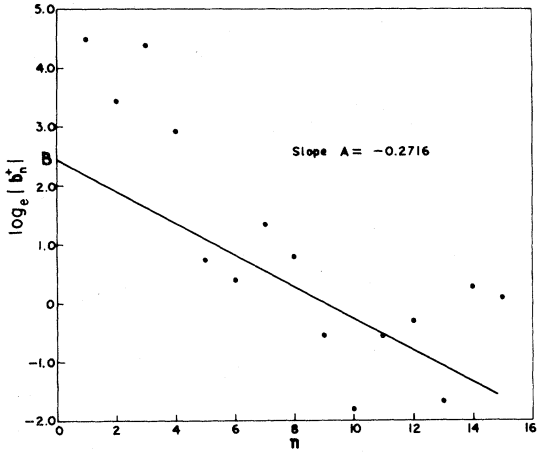

FIG. 3. Logarithm of the absolute value of the coefficients of the polynomial expansion of Eq. (32) versus the order of the polynomial at 68 MeV in the z plane. The average slope is obtained for $n\sim5$ to 14.

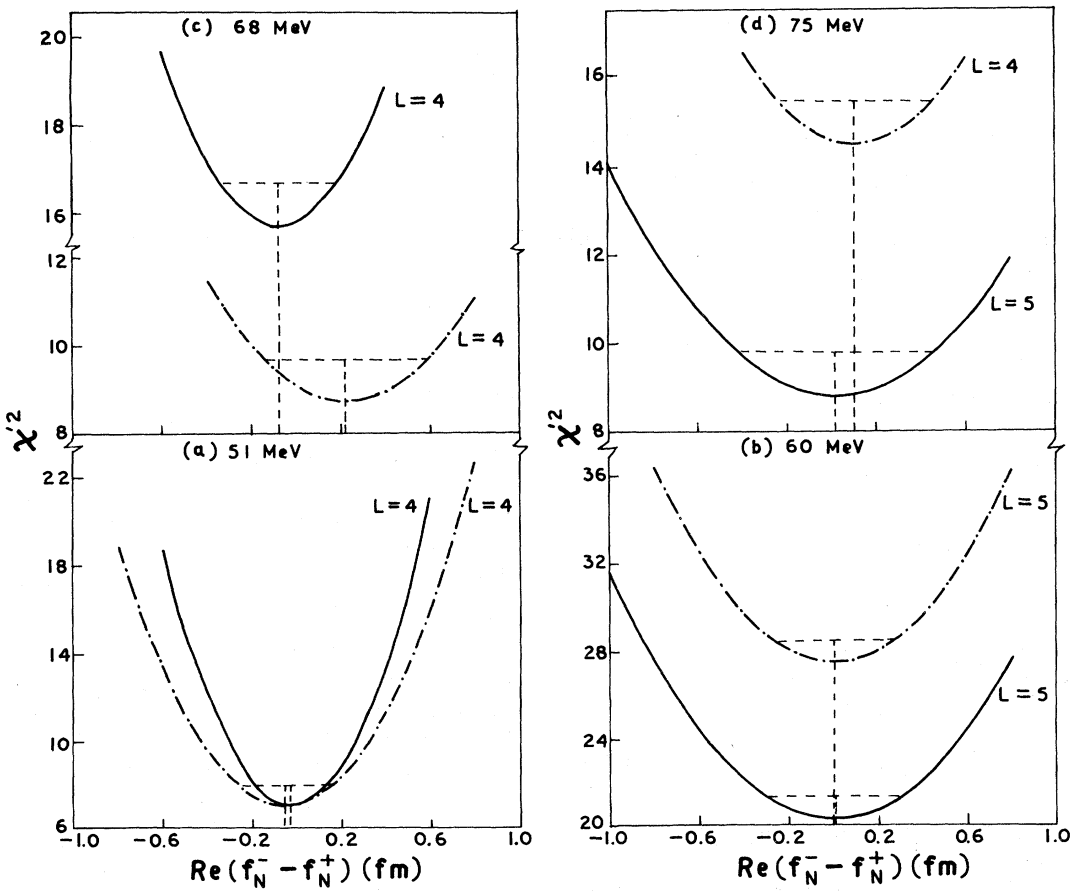

FIG. 4. Plot of χ'^2 against different values of $\mathrm{Re}[f_N^-(0)-f_N^+(0)]$. Solid curves for the x plane; dotted-dashed curves for the z plane. χ'^2 is obtained from the fit after subtraction of the ideal series (see text).

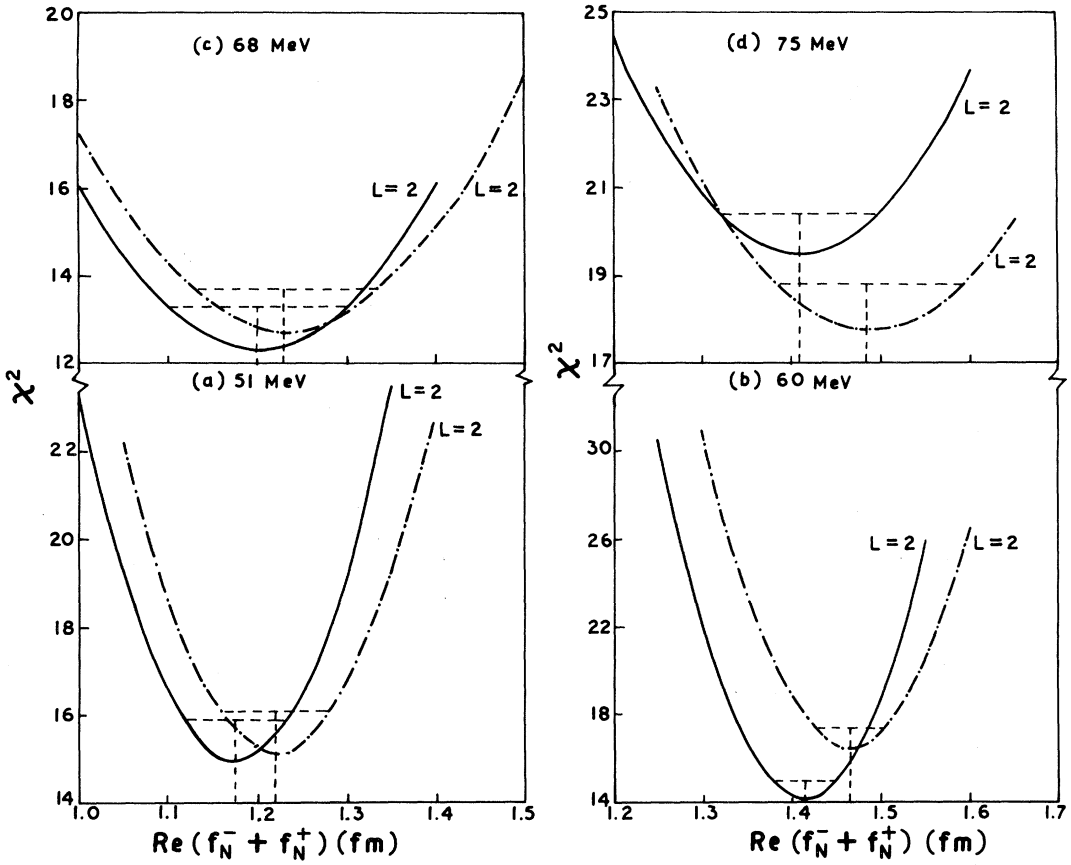

FIG. 5. Plot of χ^2 against different values of $\mathrm{Re}[f_N^-(0)+f_N^+(0)]$. Solid curves for the x plane; dotted-dashed curves for the z plane.

have the polynomial expansion

$$\mathscr{F}_+(s,\theta)=\frac{d\sigma_N^-}{d\Omega}(\theta)+\frac{d\sigma_N^+}{d\Omega}(\theta)$$

$$=\sum_n b_n^+ P_n(z)\,, \tag{32}$$

or

$$\mathscr{F}_-(s,\theta)=\frac{d\sigma_N^-}{d\Omega}(\theta)-\frac{d\sigma_N^+}{d\Omega}(\theta)$$

$$=\sum_n b_n^- P_n(z)\,. \tag{33}$$

A variation in the residues of the last terms of Eqs. (30) and (31) changes the χ^2 value insignificantly. This is to be expected since they contain α in second order. For this reason we conveniently take some approximate values for $[\mathrm{Im}f_N^-(0)+\mathrm{Im}F_N^+(0)]$ and $[\mathrm{Im}f_N^-(0)-\mathrm{Im}f_N^+(0)]$ and carry out the extrapolation with different values for $[\mathrm{Re}f_N^-(0)-\mathrm{Re}f_N^+(0)]$ and $[\mathrm{Re}f_N^-(0)+\mathrm{Re}f_N^+(0)]$. χ^2 values show sharper minima in the latter case. The values of the sum of the real parts at forward angles are thus quite accurately obtained. The sum and the difference given by Eqs. (32) and (33), when extrapolated to all angles through the polynomials, yield $d\sigma_N^\pm/d\Omega(0°)$ and $\sigma_{\mathrm{el}}^\pm$. For elliptic mapping, we have ignored the small difference between the left-hand cuts for positive and negative pions.

$\chi^2_{\mathrm{min/NDF}}$ for the fits are given in Tables IV and V. It can be noticed that $\chi^2_{\mathrm{min/NDF}}$ obtained for the fits of the difference of scattering cross sections are quite acceptable, whereas for the fits of the sum of the cross sections, we get large values of $\chi^2_{\mathrm{min/NDF}}$. This is due to inability of the pole terms to be visible against the background as the higher order polynomials contribute significantly to the χ^2 of the fit. This difficulty has been circumvented by constructing an ideal series from the ansatz that the b_n^+'s de-

TABLE III. Results of pole extrapolation for the π^--^{4}He scattering cross-section data of Binon *et al.*; values within the parentheses are calculated from phase shifts obtained by Binon *et al.*; NDF=number of degrees of freedom.

T^{lab} (MeV)	$\text{Re}f_{\bar{N}}(0)$ (fm)	$\frac{d\sigma_{\bar{N}}}{d\Omega}(0°)$ (mb/sr)	$\text{Im}f_{\bar{N}}(0)$ (fm)	σ_{tot}^{-} (mb)	σ_{el}^{-} (mb)	σ_{inel}^{-} (mb)	L, χ^2/NDF
			x plane				
110	1.197 ±0.063	45.65 ±1.05	1.769 ±0.013	225.99 ±1.69	75.55 ±0.70	150.44 ±1.86	7, 0.98
150	0.565 ±0.350	94.50 ±3.50	3.021 ±0.007	317.69 ±0.79	111.55 ±2.45	206.14 ±2.57	8, 0.99
180	0.165 ±0.115	116.90 ±2.20	3.415 ±0.026	319.14 ±2.43	111.10 ±1.05	208.04 ±2.65	9, 1.14
220	0.140 ±0.560	121.80 ±3.70	3.487 ±0.032	285.28 ±2.62	104.00 ±2.30	181.28 ±3.48	9, 1.51
260	−0.960 ±0.085	113.05 ±1.30	3.222 ±0.045	235.39 ±3.29	84.90 ±0.55	150.49 ±3.33	10, 0.92
			z plane				
110	1.20 ±0.06 (1.097)	45.65 ±0.85 (46.86)	1.767 ±0.016 (1.866)	225.84 ±2.04	75.65 ±0.70	150.19 ±2.16	5, 0.96
150	0.51 ±0.37 (0.532)	95.50 ±3.80 (93.11)	3.048 ±0.0004 (3.004)	320.52 ±0.04	111.60 ±2.55	208.92 ±2.55	6, 0.99
180	0.135 ±0.125 (−0.017)	117.55 ±2.55 (117.38)	3.426 ±0.032 (3.426)	320.16 ±3.02	111.08 ±1.13	209.08 ±3.22	7, 1.20
220	−0.45 ±0.70 (0.014)	128.70 ±6.20 (118.58)	3.557 ±0.175 (3.443)	291.06 ±14.32	106.90 ±3.10	184.16 ±14.65	7, 1.39
260	−0.970 ±0.105 (−0.899)	112.90 ±2.00 (103.34)	3.217 ±0.062 (3.086)	235.03 ±4.53	84.98 ±0.58	150.05 ±4.57	8, 0.88

crease exponentially for large n values.[12] This is explained below.

The ideal series $\sum_{n=1}^{N} C_n P_n(z)$, N being the number of data points, is constructed with the weighted polynomials $P_n(z)$ such that the coefficients C_n are close to b_n^+'s of Eq. (32) in higher order with n around three to five, but fall off exponentially with increasing n. This is done by plotting a graph of $\log_e | b_n^+ |$ against n and taking an average slope A for suitably chosen n values. The corresponding intercept B on the $\log_e | b_n^+ |$ axis enables us to construct coefficients of an ideal series,

$$| C_n | = \exp(An + B) . \tag{34}$$

In the ideal series, C_n's are required to carry the same signs as those of b_n^+'s. Subtracting this ideal theoretical series, i.e., $\sum_{n=1}^{N} e^{An+B} P_n(z)$, from the experimental cross sections, a fit to the polynomial expansion is made. The χ'^2 values are much lower, as is to be expected.

To illustrate the above process, consider the analysis of the data at 68 MeV for which a normal polynomial fit has yielded a χ^2/NDF (number of degrees of freedom) of 1.85 in the z plane for $L=4$.

TABLE IV. Results of pole extrapolation from the sum of the differential scattering cross-section data of Crowe *et al.* for π^+ and π^-. χ'^2 is obtained from the fit after subtraction of the ideal series (see text).

T^{lab} (MeV)	$\text{Re}[f_N^-(0)-f_N^+(0)]$ (fm)	$\left[\frac{d\sigma_N^-}{d\Omega}+\frac{d\sigma_N^+}{d\Omega}\right]_{\theta=0^\circ}$ (mb/sr)	$\sigma_{\text{el}}^-+\sigma_{\text{el}}^+$ (mb)	L, χ^2/NDF	L, χ'^2/NDF
		x plane			
51	−0.03±0.17	9.65±0.70	57.2±1.8	4, 2.04	4, 0.64
60	0.0 ±0.30	15.80±1.90	71.0±3.2	5, 6.35	5, 2.04
68	−0.06±0.26	17.55±1.00	77.0±2.2	5, 2.32	4, 1.43
75	0.02±0.22	25.60±1.80	91.2±3.6	5, 4.36	5, 0.88
		z plane			
51	−0.05±0.21	10.80±1.10	58.0±2.6	4, 2.09	4, 0.64
60	0.01±0.27	15.60±1.60	70.9±2.9	5, 5.34	5, 2.75
68	0.22±0.34	19.35±1.65	77.4±3.4	4, 1.85	4, 0.80
75	0.11±0.33	26.90±1.30	91.1±2.7	4, 3.18	4, 1.31

The plot of $\log_e |b_n^+|$ against n is shown in Fig. 3. The average slope A of this for $n\sim5$ to 14 is −0.2716. Its intercept B is 2.447. The ideal series now is

$$\sum_{n=1}^{N} \exp(-0.2716n+2.447)P_n(z)$$

and the signs of C_n's are the same as those of b_n^+'s for the same n value. This series is subtracted from Eq. (30). Then a fit to the polynomial expansion $\sum_n b_n P_n(z)$ is carried out. The subtraction method yields $\chi'^2/\text{NDF}=0.80$.

The χ'^2 curves so obtained for all lower energies are shown in Fig. 4. Figure 5 displays the χ^2 curves for the normal polynomial fit of the difference of differential cross sections of π^+ and π^-.

VI. RESULTS AND DISCUSSION

The results of our analysis are given in Tables III–VII. The errors correspond to a variation of χ^2 from χ_{min}^2 to χ_{min}^2+1. The elliptic mapping

TABLE V. Results of pole extrapolation from the difference of the differential scattering cross-section data of Crowe *et al.* for π^+ and π^-.

T^{lab} (MeV)	$\text{Re}[f_N^-(0)+f_N^+(0)]$ (fm)	$\left[\frac{d\sigma_N^-}{d\Omega}-\frac{d\sigma_N^+}{d\Omega}\right]_{\theta=0^\circ}$ (mb/sr)	$\sigma_{\text{el}}^--\sigma_{\text{el}}^+$ (mb)	L, χ^2/NDF
		x plane		
51	1.175±0.055	−1.47 ±0.09	−7.67 ±0.29	2, 1.15
60	1.415±0.035	−1.435±0.06	−7.10 ±0.14	2, 1.08
68	1.200±0.100	−0.93 ±0.11	−5.80 ±0.35	2, 0.95
75	1.410±0.085	−1.03 ±0.09	−5.14 ±0.26	2, 1.49
		z plane		
51	1.220±0.060	−1.66 ±0.12	−8.36 ±0.36	2, 1.16
60	1.465±0.040	−1.625±0.06	−7.90 ±0.16	2, 1.26
68	1.230±0.100	−1.04 ±0.14	−6.225±0.40	2, 0.98
75	1.485±0.105	−1.235±0.12	−5.82 ±0.34	2, 1.37

TABLE VI. Results of pole extrapolation from differential cross-section data of Crowe *et al.*; values within the parentheses are calculated from phase shifts obtained by Binon *et al.*

T^{lab} (MeV)	$\mathrm{Re}f_N^-(0)$ (fm)	$\mathrm{Re}f_N^+(0)$ (fm)	$\frac{d\sigma_N^-}{d\Omega}(0°)$ (mb/sr)	$\frac{d\sigma_N^+}{d\Omega}(0°)$ (mb/sr)	$\mathrm{Im}f_N^-(0)$ (fm)	$\mathrm{Im}f_N^+(0)$ (fm)
			x plane			
51	0.572 ±0.089	0.602 ±0.089	4.09 ±0.35	5.56 ±0.35	0.286 ±0.117	0.439 ±0.082
60	0.707 ±0.150	0.707 ±0.150	7.18 ±0.95	8.62 ±0.95	0.467 ±0.125	0.601 ±0.097
68	0.570 ±0.139	0.630 ±0.139	8.31 ±0.50	9.24 ±0.50	0.711 ±0.076	0.726 ±0.086
75	0.715 ±0.118	0.695 ±0.118	12.29 ±0.90	13.32 ±0.90	0.847 ±0.046	0.921 ±0.040
			z plane			
51	0.585 ±0.109 (0.639)	0.635 ±0.109 (0.637)	4.57 ±0.55 (4.94)	6.23 ±0.55 (5.20)	0.338 ±0.108 (0.290)	0.468 ±0.090 (0.337)
60	0.737 ±0.136 (0.744)	0.727 ±0.136 (0.733)	6.99 ±0.80 (7.73)	8.61 ±0.80 (8.07)	0.394 ±0.152 (0.467)	0.576 ±0.102 (0.518)
68	0.725 ±0.186 (0.733)	0.505 ±0.186 (0.714)	9.16 ±0.83 (9.35)	10.20 ±0.83 (9.73)	0.624 ±0.149 (0.630)	0.874 ±0.060 (0.680)
75	0.797 ±0.173 (0.812)	0.687 ±0.173 (0.784)	12.83 ±0.65 (13.33)	14.07 ±0.65 (13.83)	0.805 ±0.130 (0.820)	0.966 ±0.089 (0.875)

has helped remarkably in improving the rate of convergence of the polynomial expansions at energies above 110 MeV. It has reduced the required number of parameters for the fit by about two everywhere, as indicated by column 8 of Table III. But the mapping does not provide much improvement in the lower energy region. Column 6 of Table IV shows that only at 75 MeV the required number of parameters decreases from five to four due to mapping. At 68 MeV, even though the number of parameters is not reduced, the χ'^2/NDF value has fallen from 1.43 to 0.8. But at energies below 60 MeV, there is no improvement at all due to mapping. Similar behavior is also noted from column 5 Table V. At 75 MeV, χ^2/NDF has been reduced from 1.49 to 1.37. But below this energy, χ^2/NDF values become worse with mapping. One possible explanation could be that at low energies, far away portions of the cut come closer to the physical region due to the elliptic mapping and spoil the goodness of the fits.

Elimination of the background contribution from the terms with $n > L$ by subtraction conspicuously reduces χ^2/NDF values, as can be seen from columns 5 and 6 of Table IV, thereby providing a better fit. At 60 MeV, even though χ'^2/NDF is a little above the acceptable value, one can notice the substantial improvement the method has provided by diminishing the ratio from 6.35 as obtained by usual polynomial fit to 2.04 in *x* plane, and from 5.34 as obtained by the usual fit to 2.75 in the *z* plane.

Figure 6 is a plot of the real part of the forward amplitude against the laboratory kinetic energy of pions. The values agree well with those obtained from Binon *et al.*[7] They also agree fairly well with those of dispersion relation calculations made by Wilkin *et al.*[2] and Batty *et al.*[3] However, at 260

TABLE VII. Total cross section, total elastic and total inelastic cross sections obtained by pole extrapolation from the data of Crowe *et al.*

T^{lab} (MeV)	σ^{-}_{tot} (mb)	σ^{+}_{tot} (mb)	σ^{-}_{el} (mb)	σ^{+}_{el} (mb)	σ^{-}_{inel} (mb)	σ^{+}_{inel} (mb)
			x plane			
51	57.44 ±23.70	88.17 ±16.47	24.77 ±0.91	32.68 ±0.91	31.67 ±23.72	55.49 ±16.50
60	85.50 ±22.89	110.04 ±17.76	31.95 ±1.60	39.05 ±1.60	53.55 ±22.94	70.99 ±17.83
68	121.10 ±12.94	123.65 ±14.65	35.60 ±1.11	41.40 ±1.11	85.50 ±12.99	82.25 ±14.69
75	136.23 ±7.40	148.13 ±6.43	43.03 ±1.80	48.17 ±1.80	93.20 ±7.61	99.96 ±6.68
			z plane			
51	67.88 ±21.69	93.99 ±18.08	24.82 ±1.31	33.18 ±1.31	43.06 ±21.73	60.81 ±18.12
60	72.14 ±27.83	105.46 ±18.68	31.50 ±1.45	39.40 ±1.45	40.64 ±27.87	66.06 ±18.73
68	106.28 ±25.38	148.86 ±10.22	35.59 ±1.71	41.81 ±1.71	70.69 ±25.43	107.05 ±10.36
75	129.47 ±20.91	155.37 ±14.31	42.64 ±1.36	48.36 ±1.36	86.83 ±20.95	107.01 ±14.38

MeV and at higher energies both Binon's result and our result differ appreciably from the results of dispersion relation calculations. The results for π^+ are not shown in the figure to avoid overlapping.

From Table V it is obvious that even after subtraction of the "known" Coulomb term and the interference terms, the cross sections for π^+ and π^- are different. After repeated trials we have observed that this difference is real and is more conspicuous with decreasing energy. We are thus led to believe that there is considerable distortion of the nuclear amplitude at low energies due to Coulomb fields of the pion and the nucleus. Figure 7 is a plot of the total cross section, total elastic, and total inelastic cross sections versus pion kinetic energy. The results are in close agreement with those of Binon. At low energies there are large errors in σ_{tot}. The total cross section is maximum between 150–185 MeV around the energy region of the π-N $(\frac{3}{2},\frac{3}{2})$ resonance. The extrapolated cross section versus the laboratory kinetic energy is displayed in Fig. 8 for both negative and positive pions. The results are also in agreement with those of Binon for π^-.

As an additional check, we have calculated nuclear data at forward angles from the phase shifts given by Binon *et al.*[7] The values are given in Tables III and VI within brackets. It can be seen that our results of pole extrapolation agree well

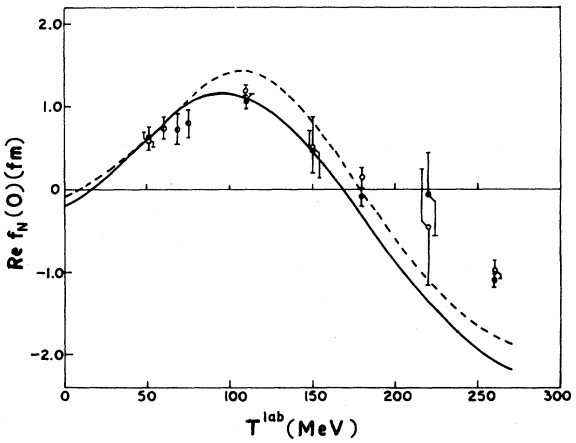

FIG. 6. Real part of forward scattering amplitude versus laboratory kinetic energy of pions. The curves were calculated from forward dispersion relation by Wilkin *et al.* (dashed curve) and by Batty *et al.* (solid curve). Results obtained by Binon *et al.* (●); results obtained by pole extrapolation (○).

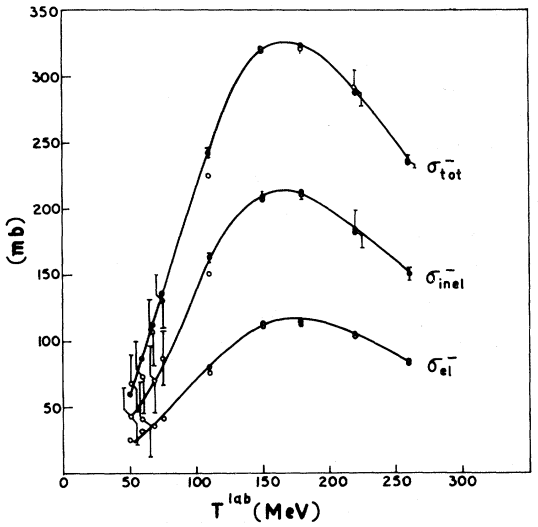

FIG. 7. π^--^{4}He total cross section, total inelastic cross section, and total elastic cross section versus pion kinetic energy. Results obtained by Binon *et al.* (●). Results obtained by pole extrapolation (○). The curves are to guide the eye only.

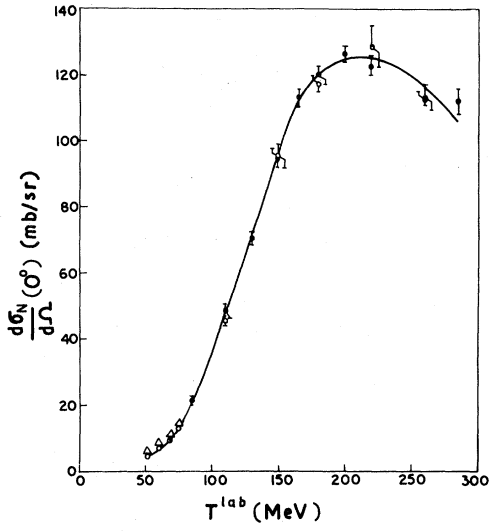

FIG. 8. Elastic differential cross section at 0° versus pion kinetic energy. Results obtained by Binon *et al.* (●); results obtained by pole extrapolation for π^- (○) and for π^+ (Δ). The solid curve is to guide the eye.

with their values. We emphasize that our results should be more reliable, as they are free from any ambiguity arising from normal phase-shift analysis.

It is worthwhile mentioning that there have been various attempts[13,18–20] for determining pion size from experiments on charged pion scattering from atomic nuclei, especially from ^{4}He. We find that our method, in the present form, cannot predict the value of r_π accurately.

More exact values of the magnitude of Coulomb distortion at low energies can be found when more accurate data, still closer to the forward region, are available. This analysis can be extended to scattering of pions from other light nuclei such as ^{12}C and ^{16}O, which will perhaps throw more light on the behavior of the Δ_{33} resonance inside a nucleus.

To summarize, we have succeeded in our purpose of presenting a model independent method for calculation of nuclear parameters in the forward region. The results obtained by the method for $\pi^\pm$-^{4}He agree with the best known values obtained so far. The conformal mapping technique has also helped in reducing the number of parameters and, at the same time, improved the goodness of the fits. Data on scattering of heavier charged nuclear objects are accumulating. Our method will help to extract the nuclear parameters without explicit knowledge of the strong nuclear amplitude.

ACKNOWLEDGMENT

We are thankful to the personnel of the Computer Centre, Utkal University, for the cooperation with the computational work. This work was supported in part by the University Grants Commission of India under the Faculty Improvement Programme.

[1]T. E. O. Ericson and M. P. Locher, Nucl. Phys. A148, 1 (1970).

[2]C. Wilkin, C. R. Cox, J. J. Domingo, K. Gabathuler, E. Pedroni, J. Rohlin, P. Schwaller, and N. W. Tanner, Nucl. Phys. B62, 61 (1973).

[3]C. Batty, G. Squier, and G. Turner, Nucl. Phys. B67, 492 (1973).

[4]I. V. Falomkin, M. M. Kulyukin, V. I. Lyashenko, A. Mihul, F. Nichitiu, T. Piragino, G. Pontecorvo, and Yu. A. Scherbakov, Joint Institute for Nuclear

Research Report E1-6534, Dubna, 1972.
[5]O. V. Dumbrais, F. Nichitiu, and Yu. A. Shcherbakov, Rev. Roum. Phys. 18, No. 10, 1249 (1973).
[6]F. Binon, V. Bobyr, P. Duteil, M. Gouanere, L. Hugon, J. P. Peigneux, J. Renuart, C. Schmit, M. Spighal, and J. P. Stroot, Nucl. Phys. B33, 42 (1971).
[7]F. Binon, P. Duteil, M. Gouanere, L. Hugon, J. Jansen, J. P. Lagnaux, H. Palevsky, J. P. Peigneux, M. Spighel, and J. P. Stroot, Phys. Rev. Lett. 35, 145 (1975); Nucl. Phys. A298, 499 (1978).
[8]M. L. Scott, G. S. Mutchler, C. R. Fletcher, E. V. Hungerford, L. V. Coulson, G. C. Phillips, B. W. Mayes, L. Y. Lee, J. C. Allred, and Clark Goodman, Phys. Rev. Lett. 28, 1209 (1972).
[9]G. B. West and D. R. Yennie, Phys. Rev. 172, 1413 (1968).
[10]L. S. Kisslinger, Phys. Rev. Lett. 29, 505 (1972); L. S. Kisslinger, Phys. Lett. 47B, 93 (1973); S. Dubnička, O. V. Dumbrais, and F. Nichitiu, Nucl. Phys. A217, 535 (1973); S. Dubnička, and O. V. Dumbrais, *ibid.* 235, 417 (1974).
[11]L. S. Kisslinger and K. Nichols, Phys. Rev. C 12, 36 (1975).
[12]R. E. Cutkosky and B. B. Deo, Phys. Rev. Lett. 20, 1272 (1968); D. Schwela, Nuovo Cimento Lett. 5, 453 (1972).
[13]K. M. Crowe, A. Fainberg, J. Miller, and A. Parsons, Phys. Rev. 180, 1349 (1969).
[14]M. L. Goldherger and K. M. Watson, *Collision Theory* (Wiley, New York, 1967), p. 263.
[15]M. D. Cooper, M. B. Johnson, and G. B. West, Nucl. Phys. A292, 350 (1977).
[16]H. Lehmann, Nuovo Cimento 10, 579 (1958).
[17]R. E. Cutkosky and B. B. Deo, Phys. Rev. 174, 1859 (1968).
[18]M. M. Sternheim and R. Hofstadter, Nuovo Cimento 38, 1854 (1965).
[19]M. E. Nordberg and K. F. Kinsey, Phys. Lett. 20, 692 (1966).
[20]F. Nichitiu and Yu. A. Shcherbakov, Nucl. Phys. B61, 429 (1973).